Cover Page

Universiteit Leiden
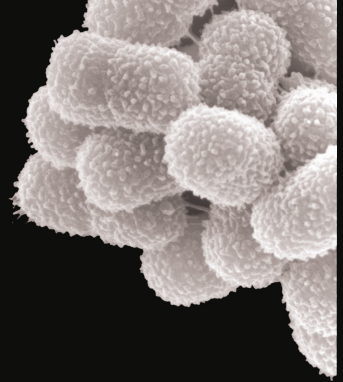
The handle http://hdl.handle.net/1887/19114 holds various files of this Leiden University dissertation.

Author: Breij, Anastasia de
Title: Towards an explanation for the success of Acinetobacter baumannii in the human host
Issue Date: 2012-06-20

Chapter 5

The clinical success of *Acinetobacter* species; genetic metabolic and virulence attributes

Anton Peleg[1,2,3], Anna de Breij[4], Mark Adams[5], Gustavo Cerqueira[1], Stefano Mocali[6], Marco Galardini[7], Peter Nibbering[4], Ashlee Earl[8], Doyle Ward[8], David Paterson[9], Harald Seifert[10], Lenie Dijkshoorn[4]

[1]Dept. of Microbiology, Monash University, Melbourne, Australia, [2]Dept. of Infectious Diseases, Alfred Hospital, Melbourne, Australia, [3]Division of Infectious Diseases, Beth Israel Deaconess Medical Center, Boston, MA, USA, [4]Dept. of Infectious Diseases, Leiden University Medical Center, Leiden, the Netherlands, [5]Dept. of Genetics and Center for Proteomics and Bioinformatics, Case Western Reserve University, Cleveland, OH, USA, [6]Agrobiology and Pedology Center, Agricultural Research Council (CRA-ABP), Florence, Italy, [7]Dept. of Evolutionary Biology, University of Florence, Italy, [8]Broad Institute, Cambridge, MA, USA, [9]University of Queensland Center for Clinical Research, Royal Brisbane and Women's Hospital Campus, Brisbane, QLD, Australia, [10]Institute for Medical Microbiology, Immunology, and Hygiene, University of Cologne, Germany.

Abstract

An understanding of why certain *Acinetobacter* species are more successful in causing nosocomial infections, transmission and epidemic spread in healthcare institutions compared with other species is lacking. We used genomic, metabolomic and virulence studies to identify differences between *Acinetobacter* species. Fourteen strains representing nine species were examined. Genomic analysis of six strains showed that the *A. baumannii* core genome contains many genes important for diverse metabolism and survival in the host. Few were unique compared to less clinically successful species. In contrast, when the accessory genome of an individual *A. baumannii* strain was compared to a less successful species (*A. calcoaceticus*), many unique operons with putative virulence function were identified, including the *csu* operon, the acinetobactin chromosomal cluster, and bacterial defence mechanisms. Metabolomic studies showed that compared to *A. calcoaceticus* (RUH2202), *A. baumannii* ATCC 19606^T was able to utilise nitrogen sources more effectively and was more tolerant to pH, osmotic and antimicrobial stress. Virulence differences were also observed, with *A. baumannii* ATCC 19606^T, *A. pittii* SH024, and *A. nosocomialis* RUH2624 persisting and forming larger biofilms on human skin than *A. calcoaceticus*. *A. baumannii* ATCC 19606^T and *A. pittii* SH024 were also able to survive in a murine thigh infection model, whereas the other two species were eradicated. The current study provides clues to the elucidation of differences in clinical relevance among *Acinetobacter* species.

Introduction

In contemporary medicine, certain *Acinetobacter* species have proven to be highly successful in their ability to cause outbreaks and develop antibiotic resistance [1,2]. However, great diversity exists in the clinical importance of the various species, with some being dominant as human pathogens and others merely acting as colonizing or environmental organisms [2]. To date, with the recent description of the novel species *Acinetobacter pittii* (former name *Acinetobacter* genomic species [gen. sp.] 3) and *Acinetobacter nosocomialis* (former name *Acinetobacter* gen. sp. 13TU) [3], the genus *Acinetobacter* comprises 26 validly named species and 9 DNA–DNA hybridization groups (gen. sp.) with provisional designations. *A. baumannii* has long been considered the most clinically important species, with the greatest number of healthcare–related outbreaks and reports of multidrug resistance. More recently, and likely as a consequence of improved laboratory identification, *A. pittii* and *A. nosocomialis* have also surfaced as clinically significant, with increasing reports of outbreaks and antibiotic resistance [4,5,6,7,8,9]. Species that have less commonly been associated with human disease include *A. lwoffii*, *A. junii*, and *A. haemolyticus*, and some species have only been identified as colonizing human skin or very rarely described as causing human disease, such as *A. johnsonii* and *A. radioresistens* [2,7]. To our knowledge, *A. calcoaceticus* has never been implicated in serious human disease [2]. However, given the difficulty in phenotypically differentiating it from *A. baumannii*, *A. pittii* and *A. nosocomialis*, these species are often grouped together in diagnostic microbiology laboratories as the '*A. calcoaceticus* – *A. baumannii* complex'.

Thus far, the attributes that make one *Acinetobacter* species more adept at causing human outbreaks and disease than another are poorly understood. Previous studies have shown that *A. baumannii* has the ability to survive in both wet and dry conditions in the hospital environment [10,11,12]. A recent clinical study showed that relative to *A. nosocomialis*, *A. baumannii* was an independent predictor of mortality [5]. A variety of virulence mechanisms have been identified in *A. baumannii*, including siderophore–mediated iron acquisition systems, biofilm formation, adherence and outer membrane protein function, the lipopolysaccharide (LPS), capsule formation, and quorum–sensing [13]. Significantly less is understood about the non–*baumannii* species. In this study, we used a systems biology approach involving genomics, phenomics and virulence studies, to identify species characteristics that may explain why some *Acinetobacter* species are successful as human pathogens and others are not. This work deepens our understanding of *Acinetobacter* biology, which is critical to develop improved

diagnostic, preventative and therapeutic strategies against this troublesome human pathogen.

Materials and Methods

Bacterial strains and culture conditions

The 14 strains included in this study are shown in Table 1. The genomes of eight strains were sequenced in the present investigation, while for six strains, the publicly available genomes were used (Table 1). Cultures were performed at 30°C or 37°C on sheep blood agar plates (bioMérieux, Boxtel, The Netherlands) or in Luria–Bertani (LB) broth.

Whole genome sequencing

Genomic DNA was extracted using the Invitrogen Easy–DNA kit (Invitrogen, CA, USA) or as described by Boom et al. [32]. Genomes were sequenced using 454 FLX pyrosequencing (Roche) with DNA standard fragment and 3 kb jumping libraries according to the manufacturer's recommendations [33]. Genomes were assembled using Newbler and the runAssembly script was then used to assemble reads into contigs. Final assemblies were BLASTed to the NCBI non-redundant database and UniVecCore was used to remove any contaminating sequence. For annotation, *ab initio* gene models were predicted using GeneMark, Glimmer3, MetaGene, and Zcurveb (Delcher et al, Nucleic Acids Res 27, 1999; Guo et al, Nucleic Acids Res 27, 2003; Noguchi et al, Nucleic Acids Res 34, 2006). An evidence-based approach constructed open reading frames (ORFs) from BLASTX hits with the NCBI non–redundant protein database; all BLAST hits with e–values better than 1 x 10^{-10} were used as BLAST evidence. A summary of gene finding data for each locus can be viewed at the Broad Institute *Acinetobacter* group database (http://www.broadinstitute.org/annotation/genome/Acinetobacter_group/GenomeStats.html).

Phylogenetic analysis and comparative genomics

Predicted proteins from each *Acinetobacter* genome were compared using an all–against–all BLAST search and *Pseudomonas aeruginosa* PAO1 was used as the outgroup. Reciprocal best blast matches (RBM), regardless of percent identity, were stored in a custom MySQL relational database to facilitate identification of orthologous groups shared by selected phylogenetic and phenotypic groups of organisms. RBM matching proteins were clustered using the Markov clustering algorithm implemented in MCL [34], and clusters with one protein per genome were defined. These represent orthologous core genes that are

present as a single copy in each genome. The protein sequences for each cluster were aligned using CLUSTALW [35] and the resulting multiple sequence alignments were concatenated for tree building. A neighbour joining (NJ) tree was made using MEGA4 [36] and evaluated using 100 bootstrap replicates. The criteria used to define an operon were (*i*) genes were consecutive, (*ii*) genes were transcribed in the same orientation, (*iii*) the intergenic distance between the genes was no longer than 150 bp, and (*iv*) gene length was at least 450 bp [37,38].

Table 1. Characteristics of bacterial strains used in this study

Species	Strain	Origin (Place, year)	Source	Genome Size (Mb)	No. of Genes	Reference	Genbank Accession No.
A. baumannii [1]	ATCC 19606[†]	Unknown, before 1949	Urine	3.97	3766	This study	ACQB0000000
A. baumannii	ATCC 17978	Unknown, ~1951	Unknown	3.98	3791	[45]	CP000521
A. baumannii	AB0057	Washington, D.C., USA,	Blood	4.05	3853	[46]	CP001182
A. baumannii	AB307–0294	Buffalo, NY, USA, 1994	Blood	3.76	3458	[46]	CP001172
A. baumannii	AYE	Le Cremlin–Bicêtre, FR, 2001	Urine	3.94	3607	[47]	CU459141
A. baumannii	ACICU	Rome, IT, 2005	CSF	3.90	3667	[48]	CP000863
A. calcoaceticus [1]	RUH2202	Malmoe, SE, 1980–82	Wound	3.88	3566	This study	ACPK00000000
A. pittii [1]	SH024	Cologne, DE, 1993	Skin	3.97	3689	This study	ADCH0000000
A. nosocomialis [1]	RUH2624	Rotterdam, NL, 1987	Skin	3.87	3631	This study	ACQF00000000
A. lwoffii	SH145	Cologne, DE, 1994	Skin	3.48	3134	This study	ACPN0000000
A. junii	SH205	Cologne, DE, 1994	Skin	3.46	3186	This study	ACPM0000000
A. radioresistens	SH164	Cologne, DE, 1994	Skin	3.16	2874	This study	ACPO0000000
A. johnsonii	SH046	Cologne, DE, 1994	Skin	3.69	3363	This study	ACPL00000000
A. baylyi	ADP1	Atlanta, GA, USA, before 1958	Soil	3.60	3325	[49]	CR543861

DE, Germany; FR, France; IT, Italy, NL, The Netherlands; SE, Sweden; US, United States
[1]Representative strains of the *A. calcoaceticus-A. baumannii* complex that were analysed in detail.

Metabolic profiling

To assess for metabolic differences between *Acinetobacter* species, we used Phenotype Microarrays (PM) as described previously by Biolog Inc. (Hayward, CA, USA) [39]. This technology uses tetrazolium violet irreversible reduction to formazan as a reporter of active metabolism. Twenty 96–well microarray plates were used (PM 1-20) comprising 1920 different metabolic and toxic compound conditions, including 192 assays of C-source metabolism (PM 1–2), 384 assays of N–source metabolism (PM 3, 6 – 8), 96 assays of P-source and S–source metabolism (PM 4), 96 assays of biosynthetic pathways (PM 5), 96 assays of ion effects and osmolarity (PM 9), 96 assays of pH effects (PM 10), and sensitivity to 240 chemicals (PM 11–20) (Bochner, FEMS Microbiol Rev 33, 2009). In brief, a standardized bacterial cell density suspension containing a tetrazolium redox dye (measures cell respiration) was transferred into wells of the microplates, which contained dried nutrients or chemicals to create the unique culture conditions. Plates were incubated at 37°C and metabolic activity was measured colorimetrically using the redox dye (Bochner, FEMS Microbiol Rev 33, 2009). Bioinformatic software (OmniLog V. 1.5) quantified metabolism as a color–coded kinetic graph. Two independent experiments

chapter 5

were performed for all analyses. A best blast hit approach was used to map all the proteins in the four genomes to the KEGG reactions database using the KEGG proteome database (http://www.genome.jp/kegg/, release 54.1); an E–value threshold of $1x10^{-50}$ was applied. Phenotype microarray data was analyzed using GenoPhenomicon: the activity of each well was predicted as *active/not active* using a support vector machine (SVM) predictor built using SVMpython v.2 (http://www.tfinley.net /software/svmpython2/), using a training dataset of 800 manually validated samples. Relationships between genome content and phenotype microarray data were then inspected.

The analysis of PM data was carried out on the raw data–set provided by Biolog Inc., obtained by three replicates of each substrate. Binary coefficients (1/0) for positive metabolism (1) or no metabolic activity (0) were attributed to each PM well and a matrix of binary vectors, each representing a single *Acinetobacter* species, was prepared as previously described [40]. Binary data were then used to compute a similarity matrix by using Jaccard coefficient with the software PAST [41].

Growth on human skin equivalents

Human keratinocytes were isolated from fresh mamma reduction surplus skin as previously described [42]. Human epidermal skin constructs were generated as described previously [51]. In brief, human epidermal skin constructs were incubated with 300 µl of a mid–logarithmic bacterial suspension ($3x10^5$ colony forming units [CFU]/ml) at 37ºC (7.3% CO_2). After 1 h, skin constructs were washed with phosphate buffered saline (PBS) to remove non–adherent bacteria and were incubated for an additional 23 h and 47 h. Two circular biopsies (4 mm in diameter) were taken from the skin, homogenized in PBS and serially diluted to determine the number of CFU. A third biopsy of each skin construct was fixed in 4% formaldehyde, dehydrated and embedded in paraffin for subsequent staining with Alcian–blue PAS (Merck, Darmstadt, Germany) for morphological analysis. Three independent experiments were performed.

Bronchial epithelial cell adhesion and cytokine production

Adherence of bacteria to human bronchial epithelial cells (H_{292} cells, ATCC CRL–1848, Manassas, VA, USA) and cytokine production by these cells was determined as described previously [30,43]. In brief, H_{292} cells were incubated for 1 h at 37°C with $1x10^8$ CFU of an overnight bacterial culture on blood agar. Bacterial adherence to H_{292} cells was quantified by light microscopy and the average number of bacteria per 100 epithelial cells was recorded. Two independent experiments were performed in duplicate. For cytokine production, H_{292} cells were washed five times after 1 h of bacterial infection (as described

above) with prewarmed PBS, and fresh RPMI medium was added. After 23 h incubation at 37°C, supernatants were collected and stored at –20°C until determination of cytokine levels. RPMI medium alone was used as a control. Interleukin (IL)–6 and IL–8 were determined by enzyme–linked immunosorbent assays (ELISA, Biosource, CA, USA) according to the manufacturer's instructions. The lower limit of detection was 15 pg/ml for IL–6 and 7 pg/ml for IL–8. Three independent experiments were performed.

Murine thigh infection model

The survival of *Acinetobacter* strains in a mouse thigh muscle infection model was assessed as previously described [44], with modifications. Female Swiss mice (Charles River Nederland, Maastricht, The Netherlands) were made transiently neutropenic by intraperitoneal injection with cyclophosphamide (150 mg/kg body weight in 150 µl) on day 4 and 3 prior to infection. Approximately $1x10^4$ CFU (in 50 µl of saline) of a mid–logarithmic culture was injected in the right thigh muscle (three animals per strain). At 48 h after infection, mice were sacrificed and infected thigh muscles were removed and homogenized in 1 ml PBS and viable counts were performed. The animal studies were approved by the Leiden Experimental Animal Committee (Permit number: 10038) and were performed in compliance with Dutch laws related to the conduct of animal experiments. All efforts were undertaken to minimize suffering.

Statistical analysis

All data were analysed for statistical significance using the Wilcoxon rank sum test. *P* values of ≤ 0.05 were considered statistically significant.

Results

**Genome characteristics of the *Acinetobacter* species**

As shown in Table 1, 14 genomes were included in this analysis, covering nine different *Acinetobacter* species (species names will be used for non–*baumannii* species throughout). Eight strains were sequenced as part of this study with mean coverage of 22–fold. Overall, the species that make up the *A. calcoaceticus – A. baumannii* complex had the largest genomes, with *A. radioresistens* having the smallest (3.16 Mb). Genome sizes of strains within the *A. baumannii* species varied by up to 289 Kb. The number of genes corresponded to genome size, ranging from 3,690 in *A. baumannii* to 2,874 in *A. radioresistens*. Phylogenetic analysis showed that the species that make up the *A. calcoaceticus – A. baumannii* complex were most closely related, with *A. nosocomialis*

chapter 5

being closest to *A. baumannii*, followed by *A. pittii* and *A. calcoaceticus* (Figure S1). The other species formed distinct phylogenetic branches (Figure S1).

Analysis of the *A. baumannii* core genome

To understand the genetic core of *A. baumannii*, we first analysed the orthologous genes found in all six *A. baumannii* genomes. This analysis yielded 2,800 genes, indicating that the accessory genome varied between 658 – 1,053 genes depending on the strain. A distribution of the *A. baumannii* core genome based on functional gene categories is shown in Figure 1. Apart from genes of general or unknown function, genes related to molecule transport and metabolism were most abundant (35%), including amino acid (11%), carbohydrate (5%), lipid (5%), nucleotide (3%), coenzyme (4%) and inorganic ion (7%) processing.
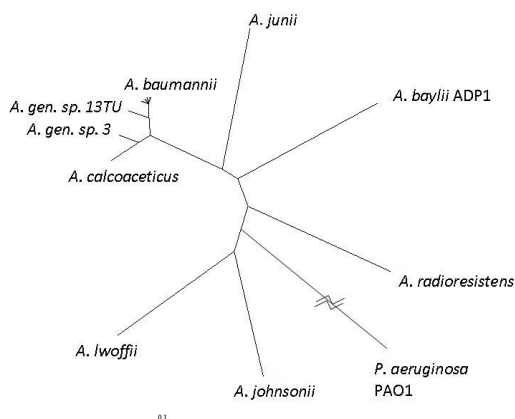

Figure S1. Phylogenetic analysis of the eight sequenced strains of *Acinetobacter* species from this study.

Interestingly, despite *Acinetobacter* deriving its name from akineto meaning non–motile, *A. baumannii* has several core cell motility genes. These include a type IV pilus apparatus and pilus assembly genes (*pilB*, *pilW*, *pilL*, *pilJ*, *pilI*, *pilY1*, *pilQ*, *pilO*, *pilN*, *pilM*), fimbrial biogenesis genes (*fimT*, *pilZ*), and twitching motility genes (*pilU*, *pilT*, which are important for pilus retraction). In fact, it has recently been shown that *A. baumannii* is motile under certain conditions [14,15], and this may play an important role in its ability to colonize and spread on surfaces, and to form biofilms [16]. We also identified 24 genes that appear to determine *A. baumannii* cell shape and division, including the cell division genes (*ftsA*, *ftsZ*, *ftsW*, *ftsK*), the rod shape determining genes (*mreB*, *rodA*) and the *min* operon (*minE*, *minD*, *minC*), which controls the position in which FtsZ assembles in the center of the cell.

Given that cell division biosynthetic machinery has been targeted in other successful antibacterial therapies, the identification of these genes is promising [17].
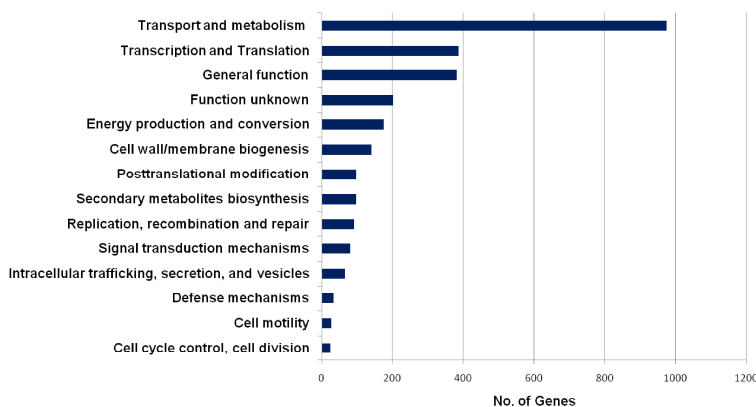
Figure 1. *A. baumannii* core genome. Functional distribution of the genes found in all six *A. baumannii* strains included in this study.

Comparison of *A. baumannii* genome with other *Acinetobacter* species

To begin to decipher the genetic attributes that may help explain why some *Acinetobacter* species are clinically more significant than others, we assessed for genes observed uniquely in pathogenic species of *Acinetobacter* (the six *A. baumannii* genomes, and the *A. pittii* and *A. nosocomialis* genome). This analysis identified 51 genes, including 12 operons, shared among these eight genomes that were not present in the other species (Table S1). Importantly, one of these operons was the *csu* operon, which includes six genes, and codes for proteins involved in a chaperone – usher pili assembly system [18]. This operon appears important for pili assembly, adherence to abiotic surfaces and biofilm formation [18]. The presence of this operon only in pathogenic species of *Acinetobacter* highlights its potential role in determining the clinical success of these species. The predominant functional categorization of the remaining genes was in molecule transport and metabolism, and transcription (Table S1).

Comparison of specific strains of the *A. calcoaceticus* – *A. baumannii* complex

The data presented thus far provide some evidence that a small number of core genes may partly explain the clinical success of certain *Acinetobacter* species; however the number of genes that differed was few, suggesting that additional genetic characteristics that distinguish pathogenic from less pathogenic strains may be found among the accessory genomes.

chapter 5

Table S1. Unique genes found in pathogenic species of *Acinetobacter* (*A. baumannii* [six strains], *A. pittii* and *A. nosocomialis*) and not in other less or non-pathogenic species

ATCC19606	Description	COG Description	Operon	Homologues (nt ID %)	
				A. pittii	*A. nosocomialis*
ACIB1v1_040004	transcriptional regulator, TetR family	Transcription	No	89.6	90.1
ACIB1v1_050001	CsuA/B	Cell motility		99.4	99.4
ACIB1v1_050002	CsuA	Cell motility		84.1	85.2
ACIB1v1_050003	CsuB	Cell motility	Yes	89.5	87.4
ACIB1v1_050004	CsuC	Cell motility		96.3	94.5
ACIB1v1_050005	CsuD	Cell motility		95.8	95.3
ACIB1v1_050006	CsuE	Cell motility		95.7	99.3
ACIB1v1_050012	transcriptional regulator, TetR family	Transcription	No	72.2	72.2
ACIB1v1_050037	acetyltransferase, gnat family	General function prediction only	No	96.0	99.3
ACIB1v1_090011	transcriptional regulator, AsnC family	Transcription	No	95.3	97.3
ACIB1v1_090012	kynureninase	Amino acid transport and metabolism		90.6	95.9
ACIB1v1_090013	proline-specific permease ProY	Amino acid transport and metabolism	Yes	90.2	96.8
ACIB1v1_090014	conserved hypothetical protein	Lipid transport and metabolism		72.0	83.8
ACIB1v1_090017	conserved hypothetical protein	Function unknown	No	79.6	89.0
ACIB1v1_150007	transcriptional regulator, GntR family	Transcription	Yes	99.2	100.0
ACIB1v1_150008	dihydroxy-acid dehydratase	Carbohydrate transport and metabolism		99.5	99.5
ACIB1v1_150009	MFS family permease	General function prediction only	Yes	99.8	99.0
ACIB1v1_150010	hypothetical protein	Function unknown		97.3	99.1
ACIB1v1_150012	conserved hypothetical protein	No COG annotation	No	92.9	97.7
ACIB1v1_150014	oxidoreductase FMN-binding	Energy production and conversion	Yes	97.8	97.6
ACIB1v1_150015	saccharopine dehydrogenase	Function unknown		95.8	96.6
ACIB1v1_150017	transcriptional regulator, MerR family	Transcription	No	91.3	97.8
ACIB1v1_150046	transcriptional regulator, LysR family	Transcription	No	97.1	97.7
ACIB1v1_150047	hypothetical protein	Function unknown	Yes	97.9	95.1
ACIB1v1_150048	hypothetical protein	Function unknown		97.4	96.0
ACIB1v1_150094	putative acid phosphatase	General function prediction only	Yes	97.8	97.2
ACIB1v1_150095	conserved hypothetical protein	No COG annotation		93.0	94.4
ACIB1v1_230050	transcriptional regulator, LysR family	Transcription	No	96.7	95.8
ACIB1v1_230051	3-oxoacyl-[acyl-carrier-protein] reductase	Lipid transport and metabolism	No	95.1	95.1
ACIB1v1_240001	conserved hypothetical protein	General function prediction only	No	87.5	93.6
ACIB1v1_240049	FAD dependent oxidoreductase	Amino acid transport and metabolism	Yes	94.8	92.5
ACIB1v1_240050	ABC transporter, permease	Inorganic ion transport and metabolism		97.7	98.8
ACIB1v1_240051	ABC transporter, ATP binding protein	Amino acid transport and metabolism		95.5	97.6
ACIB1v1_240052	2-aminoethylphosphonate ABC transport system, 1-amino-ethylphosphonate-binding protein component	Inorganic ion transport and metabolism	Yes	98.3	98.8
ACIB1v1_240053	transcriptional regulator, GntR family	Transcription		97.9	99.6
ACIB1v1_240056	acyl carrier protein phosphodiesterase	Lipid transport and metabolism	No	96.0	97.5
ACIB1v1_240122	cyanate transport protein CynX	Inorganic ion transport and metabolism	Yes	78.8	90.0
ACIB1v1_240123	guanine deaminase	Nucleotide transport and metabolism		80.6	91.3
ACIB1v1_240159	glutathione-dependent formaldehyde dehydrogenase	Amino acid transport and metabolism	No	97.7	96.9
ACIB1v1_240186	4-hydroxybenzoate transporter	Amino acid transport and metabolism	No	94.5	94.5
ACIB1v1_250041	cis,cis-muconate transport protein	Amino acid transport and metabolism	No	98.9	98.6
ACIB1v1_250167	conserved hypothetical protein	No COG annotation	No	96.2	94.2
ACIB1v1_250168	transcriptional regulator, LysR family	Transcription	No	98.2	98.6
ACIB1v1_250169	tartrate dehydrogenase	Energy production and conversion	Yes	98.9	98.7
ACIB1v1_250170	betaine/choline/glycine transport protein	Cell wall/membrane/envelope biogenesis		99.3	99.5
ACIB1v1_250174	putative dioxygenase subunit beta	Energy production and conversion		95.6	97.3
ACIB1v1_430020	transcriptional regulator, TetR family	Transcription	No	93.1	93.6
ACIB1v1_460007	Peptidase M20D, amidohydrolase	General function prediction only	No	93.2	92.1
ACIB1v1_490004	TonB-dependent receptor	Inorganic ion transport and metabolism	Yes	96.2	96.8
ACIB1v1_490005	aminopeptidase N	Amino acid transport and metabolism		97.6	97.4
ACIB1v1_820017	haloacid dehydrogenase	General function prediction only	No	93.9	90.6

To interrogate the accessory genome in more detail, we analysed representative strains from the four species that make up the *A. calcoaceticus* – *A. baumannii* complex (Table 1). A distribution of genes is shown in Figure 2A. A total of 2505 genes were common to all four species, with the greatest number of unique genes observed in *A. baumannii* ATCC 19606[T]. Based on category of gene (COG) functional classification, the distribution of genes unique to *A. baumannii* ATCC 19606[T] compared to each one of the other three

strains was similar, with the greatest number of unique genes having a role in amino acid, carbohydrate and lipid transport and metabolism, and transcription (Figure 2B).
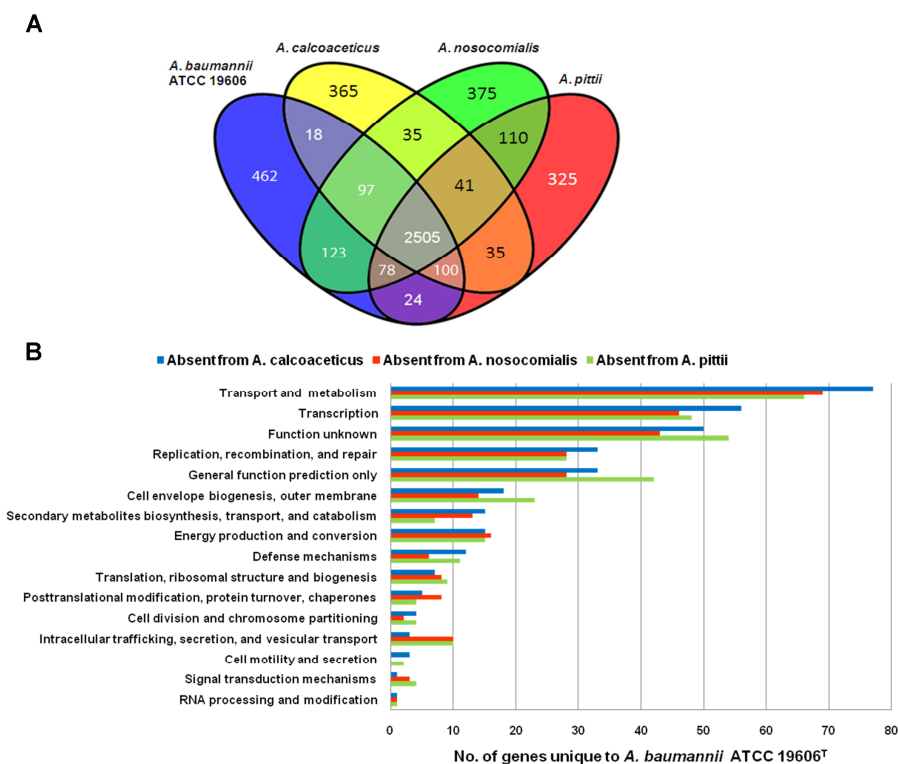
Figure 2. Distribution of genes in individual strains of the *A. calcoaceticus* – *A. baumannii* complex. (**A**) Venn diagram showing the number of overlapping genes between the four strains that make up the *A. calcoaceticus* – *A. baumannii* complex. (**B**) The number of genes present in *A. baumannii* ATCC 19606[T] but absent in each of *A. calcoaceticus*, *A. pittii* and *A. nosocomialis*.

Of most interest was the comparison between *A. baumannii* ATCC 19606[T] and *A. calcoaceticus*. This comparison identified 759 unique genes in *A. baumannii* ATCC 19606[T]. Of these, only 169 were found in the other five *A. baumannii* genomes analysed in this study, indicating that the majority of the unique genes (78%) were part of the accessory genome of *A. baumannii* ATCC 19606[T]. Of the 759 unique genes, 333 had a COG classification, and they were significantly overrepresented in several functions necessary for basic bacterial growth and survival, including transcription (56 genes), DNA replication, recombination, and repair (33 genes), amino acid, inorganic ion and carbohydrate

transport and metabolism (66 genes), and cell envelope biogenesis and outer membrane function (19 genes).

Of the 333 genes, there were 69 unique operons that were enriched in virulence–related genes, including those involved in siderophore transport and biosynthesis, LPS biosynthesis, pili and biofilm formation, Curli fimbriae assembly, and bacterial defence mechanisms (Table 2). Several operons responsible for iron handling were identified, including the acinetobactin chromosomal locus (operons 36 – 39, Table 2), encoding a key *Acinetobacter* siderophore [19,20]. The genetic organisation of this locus and homologues in *A. pittii*, *A. nosocomialis* and *A. calcoaceticus* are shown in Figure 3A. *A. calcoaceticus* and *A. nosocomialis* lacked the full complement of genes that make this locus (Table 2 and Figure 3A). We also identified a more recently described siderophore operon (operon 17, Table 2 and Figure 3B) [14], made up of eight genes, with *A. baumannii* ATCC 19606[T] being the only strain with the full complement of genes, and *A. nosocomialis* and *A. calcoaceticus* being deficient in most of them.

Table 2. Select operons with putative virulence function found in *A. baumannii* ATCC 19606[T] and not in *A. calcoaceticus*

			A. baumannii ATCC 19606[T] ORFs[1]	Homologues average similarity (ID% ± SD)[2]	
Operon ID	Function	Genes		*A . pittii*	*A. nosocomialis*
2	Pili assembly and biofilm form.	*csuAB/ABCDE*	ACIB1v1_50001–6	91.8 ± 7.1	91.8 ± 7.1
17	Siderophore transp. bios.	*cirA* , *menG* , *iucA/C*, *araJ* , *rhbE/C*	ACIB1v1_160094–101[3]	46.2 ± 17.9	31.1 ± 3.7
29	Defense mechanism	*cas1, csy1, csy2, csy3, csy4*	ACIB1v1_260071–75	–	–
36	Siderophore transp. bios.	*bauD* , *bauC* , *bauE* , *bauB* and *bauA*	ACIB1v1_480066–70	97.8 ± 1.0	–
37	Siderophore transp. bios.	*basC* and *basD*	ACIB1v1_480071–72	97.4 ± 1.0	–
38	Siderophore transp. bios.	*basE, basF, basG*	ACIB1v1_480073–75	97.6 ± 0.3	47.8 ± 0.4
39	Siderophore transp. bios.	*barA, barB, basH, basI, basJ*	ACIB1v1_480076–80	95.1 ± 6.3	32.8 ± 0.8
40	Siderophore transp. bios.	*tonB* , PEPN	ACIB1v1_490004–5	97.0 ± 0.3	97.5 ± 0.3
46	Cell motility and secretion	*pilA*	ACIB1v1_560044–45	60.2 ± 14.5	73.3 ± 0.3
47	LPS biosynthesis	*lpsC* and *lpsE*	ACIB1v1_600015–16[4]	33.9	68.2 ± 29.8
50	Curli fimbriae assembly	*csgG*	ACIB1v1_700078–80	94.8 ± 1.1	–
56	LPS biosynthesis	*wzx* , *degT* , *wbbJ* , *mviM* and *vipA*	ACIB1v1_740018–22[6]	42.6 ± 23.8	48.3 ± 17.2

Bios., Biosynthesis; Form., Formation; ID, Identity; SD, Standard Deviation; Transp., Transport.
[1]Based on Microbial Genome Annotation Platform (www.cns.fr/agc/mage) [50]. [2]Expressed as the average identity at the nucleotide level ± standard deviation. [3]Only three, two and two genes (out of eight) are found in *A. pittii*, *A. nosocomialis* and *A. calcoaceticus*, respectively. The homologues identified exhibited low similarity. [4]Both genes belong to an LPS operon that spans from ORF ACIB1v1_600009 to 16, and which is only partially present within *A. calcoaceticus* (three of eight genes are absent). [5]*lpsC* is absent from *A. pittii* genome. [6]Only *vipA* is present in *A. calcoaceticus* and exhibited moderate similarity. The operon is poorly conserved and partially present also in *A. pittii* and *A. nosocomialis*.

Unique genes related to bacterial defence mechanisms were also observed in *A. baumannii* ATCC 19606[T], including those coding for ABC transporters, and CRISPR – (Cas) and phage–related proteins. Clustered regularly interspaced short palindromic repeats (CRISPRs) are recently described adaptive bacterial immune mechanisms that protect bacteria from invading foreign genetic elements such as bacteriophages [21,22]. Such systems are likely advantageous in hostile environments, and when combined with other

phage resistance mechanisms, may provide a survival benefit to the bacterial host [21]. The *A. baumannii* ATCC 19606[T] CRISPR system includes *cas1* and *cas3*; however we could not locate *cas2*, which is thought to be required with *cas1* to form a functional CRISPR system [22]. The CRISPR operon was not found in *A. calcoaceticus*, *A. nosocomialis* or *A. pittii*.
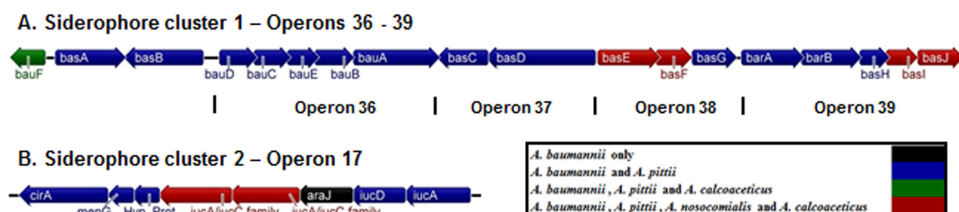

Figure 3. Genetic organisation and conservation of the siderophore clusters found in *A. baumannii* ATCC 19606[T] and not in *A. calcoaceticus*. (A) Siderophore cluster 1 (operons 36 – 39) is known as the acinetobactin chromosomal cluster, and (B) siderophore cluster 2 (operon 17) (See Table 2 for details about the operons). The presence of homologues for each gene in *A. pittii*, *A. nosocomialis*, and *A. calcoaceticus* is shown.

Comparison of the metabolic versatility of specific strains of the *A. calcoaceticus* – *A. baumannii* complex

Given the predominance of metabolism genes differentiating pathogenic and less pathogenic strains, we analyzed the metabolic profile of the four species of the *A. calcoaceticus* – *A. baumannii* complex using phenotype microarrays. Of the 1920 conditions tested, the four species shared 1356 metabolic responses (70.6%), of which 795 compounds or conditions could be utilized by all the species and 561 by none of them. A summary of the entire metabolic profile of the four species is shown in Figure 4. *A. baumannii* ATCC 19606[T] appeared to utilize peptide nitrogen sources (PM 6–8) more effectively and to be more tolerant to pH stress (PM 10) than the other three species. *A. baumannii* ATCC 19606[T] and *A. pittii* had a reduced ability to utilise most of the phosphorus and sulfur sources (PM 4) (Figure 4).

We then focused on the most clinically disparate of the species, and compared *A. baumannii* ATCC 19606[T] with *A. calcoaceticus* in more detail. In 195 conditions, *A. baumannii* ATCC 19606[T] was significantly more metabolically active than *A. calcoaceticus*. These conditions comprised 10 carbon sources, 105 nitrogen sources (of which 98 were di– and tri–peptides) and 80 stress conditions, of which 26 related to osmotic and pH stress and 54 related to the presence of antimicrobials and other cytotoxic compounds.

chapter 5
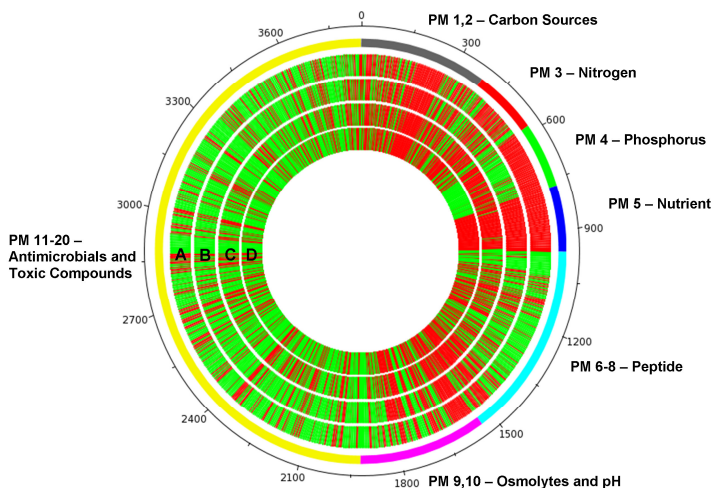
Figure 4. Metabolic diversity of specific strains of the *A. calcoaceticus – A. baumannii* complex. Phenotype Microarray (PM) comparative results showing the number of compounds used (green) or not used (red) by *A. baumannii* ATCC 19606[T] [A], *A. nosocomialis* [B], *A. pittii* [C] *and A. calcoaceticus* [D]. The external circle and PM number represent the Biolog plate number.

Apart from the likely survival advantage inferred by the greater ability of *A. baumannii* ATCC 19606[T] to metabolise in the presence of osmotic, pH and antimicrobial exposure, one of the carbon sources utilized by this strain was D–glucarate. D–glucarate is found in the human body and has been shown to be a carbon source utilized by a range of gram–negative bacteria [23,24]. D–glucarate catabolism generates α–ketoglutarate, which enhances the citric acid cycle. Recently, over–expression of the citric acid cycle was shown to occur in an *A. baumannii* strain with increased virulence in the presence of ethanol [25].

Virulence differences between strains of the *A. calcoaceticus – A. baumannii* complex
Given the differences in the number of operons with putative virulence function that were observed between the four species of the *A. calcoaceticus – A. baumannii* complex, we performed a range of in vitro and in vivo virulence studies to characterise further the functional significance of their genetic differences. Given the predilection of *A. baumannii* to colonise or infect the respiratory tract, we first analysed the interaction of the four species with human bronchial epithelial cells. Cell adherence and pro–inflammatory cytokine response (IL–8) was most pronounced with *A. pittii* ($P < 0.05$) (Figure 5, A, B and C). All strains induced similar levels of IL–6 in these cells.
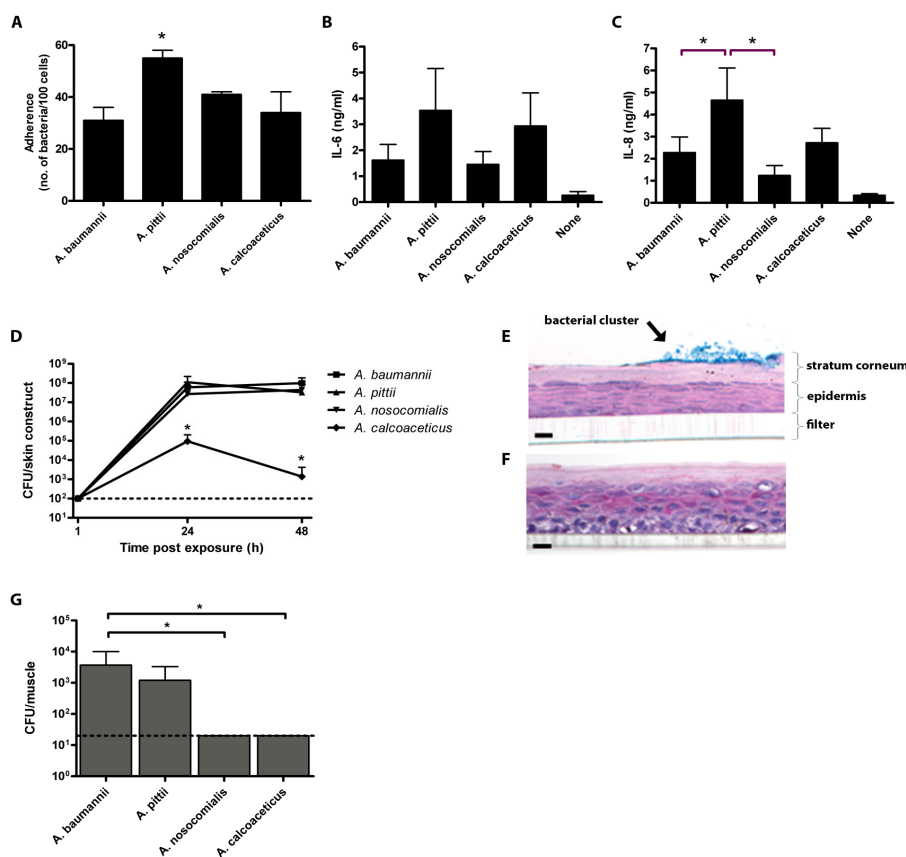
Figure 5. Virulence attributes of individual strains belonging to the *A. calcoaceticus – A. baumannii* complex. (A) Adherence of *A. baumannii* ATCC 19606[T], *A. pittii*, *A. nosocomialis* and *A. calcoaceticus* to human bronchial epithelial cells after 1 h. Results are expressed as mean number of bacteria per 100 epithelial cells ± standard deviation (SD) of two independent experiments performed in duplicate. (**B**) Levels of IL–6 and (**C**) IL–8 in the culture medium of human bronchial epithelial cells after 24 hour stimulation with specific strains of the *A. calcoaceticus – A. baumannii* complex. Results are expressed as mean levels of IL–6 and IL–8 (in ng/ml) ± SD of three independent experiments. Asterisk signifies statistical significance ($P < 0.05$). (**D**) Persistence and biofilm formation of *A. baumannii* ATCC 19606[T] (squares), *A. pittii* (upward triangles), *A. nosocomialis* (downward triangles) and *A. calcoaceticus* (diamonds) on three–dimensional human skin constructs. Results are expressed as mean CFU per skin construct ± SD of three independent experiments. Dotted line represents the lower limit of detection. (**E**) Alcian–blue PAS staining shows biofilm formation (black arrow) on human skin constructs by *A. baumannii* ATCC 19606[T] but not by (**F**) *A. calcoaceticus*. Scale bar is equivalent to 20 μm. (**G**) Approximately 1x10^{4} CFU were injected in the thigh muscles of neutropenic mice and the number of viable bacteria was determined after 48 h. Results are expressed as mean number of bacteria (in CFU/muscle) ± SD from three animals. Dotted line represents lower limit of detection. Asterisk signifies statistical significance ($P < 0.05$).

chapter 5

Given the likely importance of biofilm formation to the success of *Acinetobacter* in hospitals, we next tested the four species in a unique biofilm assay. Thus far, the correlation between biofilm formation on abiotic surfaces and clinical significance has been poor [26]. Therefore, we used a novel assay that may predict the ability of *Acinetobacter* to colonise and form a biofilm on human skin. Using a three–dimensional human skin construct [51], we observed that *A. baumannii* ATCC 19606[T], *A. pittii* and *A. nosocomialis* were able to multiply rapidly and persist on human skin, whereas *A. calcoaceticus* grew to a significantly lower density (Figure 5D). In addition, biofilms of the former three species were visible on the stratum corneum, whereas no such bacterial structures were seen for *A. calcoaceticus* (Figure 5, E and F). Finally, we assessed the survival of the four strains in a neutropenic mouse thigh muscle infection model. *A. baumannii* ATCC 19606[T] and *A. pittii* were able to survive in the thigh muscle at least up to 48 h, whereas *A. calcoaceticus* and *A. nosocomialis* were eradicated (Figure 5G).

Discussion

This study provides a combined genomic, phenomic and virulence assessment of a range of *Acinetobacter* species that have been variably associated with humans. From a genomic analysis of nine different *Acinetobacter* species, we identified a small number of genes unique to pathogenic species. The majority of these genes are predicted to be important for molecule transport and metabolism but also included the putative virulence *csu* operon. Investigating the accessory genome of individual strains of the four species of the *A. calcoaceticus – A. baumannii* complex, we found a range of unique operons with putative functions relating to host survival and virulence in *A. baumannii* ATCC 19606[T] but not in *A. calcoaceticus*. *A. pittii* appeared most similar to *A. baumannii* ATCC 19606[T], whereas *A. nosocomialis* lacked several of these important operons, particularly the full repertoire of genes of the acinetobactin chromosomal locus. Global metabolomic studies supported the genomic analysis in that *A. baumannii* ATCC 19606[T] was able to utilise more carbon and nitrogen sources, and was more tolerant to a range of cellular stresses than *A. calcoaceticus*. Moreover, the pathogenic species were able to multiply and form biofilms on human skin significantly more than *A. calcoaceticus*. Only *A. baumannii* and *A. pittii* were able to survive in a mammalian thigh infection model.

As a consequence of improved laboratory speciation, it is becoming apparent that non–*baumannii* species, particularly *A. nosocomialis* and *A. pittii*, are clinically significant human pathogens. For example, in a recent study from Norway, *A. nosocomialis* was the most common species (47%) isolated from blood cultures over a three–year period,

followed by *A. pittii* (20%) [27]. With regard to their clinical impact, a more contemporary study has shown that relative to *A. nosocomialis*, bacteremia with *A. baumannii* was an independent predictor of mortality [5]. Interestingly, and consistent with our study findings, there was no significant difference between *A. baumannii* and *A. pittii*, however the number of patients in the *A. pittii* group was small [5]. Genetically and metabolically, we showed that *A. pittii* appeared similar to *A. baumannii*, and they also behaved similarly in the mammalian infection model. *A. nosocomialis* lacked several of the virulence related operons, particularly the acinetobactin siderophore cluster, and its metabolome was more closely aligned to *A. calcoaceticus*, both of which may explain its failure to survive in the murine model and its reduced virulence in clinical studies [5].

Within mammalian hosts, free iron is often a scarce resource and for pathogenic organisms to survive in vivo they often utilize a range of iron scavenging systems. Such systems have been analysed across different *A. baumannii* strains [14,29] however this is the first analysis, to our knowledge, of such genes in non–*baumannii* species. In addition to the acinetobactin chromosomal locus, we observed another siderophore cluster and a putative iron uptake receptor in *A. baumannii* ATCC 19606[T] that was not present in *A. calcoaceticus*. This second cluster (operon 17 in Table 2) is a recently described siderophore cluster made up of eight genes that is well conserved across *A. baumannii* strains [14]. The full repertoire of genes from this cluster was not found in *A. pittii*, *A. nosocomialis*, and *A. calcoaceticus*, and the few homologues identified exhibited low similarity (Table 2). Such genetic differences between *Acinetobacter* species in key virulence attributes may help explain why some species have greater clinical impact.

Apart from genes involved in metabolism and transcription, we identified the *csu* operon as an operon found in pathogenic species of *Acinetobacter* (six *A. baumannii* strains, *A. pittii* and *A. nosocomialis*) but not in non–pathogenic species. Loss of function of this operon leads to a lack of pili–like structures on the surface of *A. baumannii* and to loss of cell attachment and biofilms on abiotic surfaces [18]. Interestingly, this operon was not shown to be important for attachment to and cytokine production by human bronchial epithelial cells [30]. We hypothesize that this operon may aid in *Acinetobacter* attachment and colonization of plastic medical devices such as ventilator tubing and catheters, with a subsequent increased risk of invasive infection. The definitive role of this operon in mammalian virulence requires further evaluation.

We observed a diverse repertoire of core metabolic genes in *A. baumannii*, which is likely to be important for its ability to survive in vivo, as well as in unique ecological niches of healthcare institutions. To assess the global metabolic capabilities of the *Acinetobacter* species, we used phenotype microarrays, which enabled us to assess nearly 2000 metabolic and toxic compound conditions. Overall, *A. baumannii* ATCC 19606[T] was

chapter 5

able to utilize nitrogen sources more effectively and was more tolerant to pH stress than *A. nosocomialis*, *A. pittii* and *A. calcoaceticus*. The differences were more marked when *A. baumannii* ATCC 19606^T was compared to *A. calcoaceticus*. Interestingly, *A. baumannii* and *A. pittii* were unable to utilize most of the phosphorus sources despite both strains having the necessary genetic composition for phosphate metabolism. Several studies have highlighted the key role of the Pho regulon in phosphate management, virulence and stress response [31]. Whether the inability of *A. baumannii* and *A. pittii* to utilize phosphorus is linked to expression of the Pho regulon remains a question that needs further evaluation.

Taken together, these data provide a systems biology approach to understanding the potential differences between important species of the *Acinetobacter* genus. We provide genetic and metabolic insights into why some species may be more clinically important than others, and also highlight the functional significance of these differences in various virulence models. A limitation of our study is that we only analysed one strain for each of the non-*baumannii* species, and our results need confirmation using a larger set of strains. Furthermore, confirmation of our findings using targeted gene deletion and complementation is required to define the significance and role of the unique operons found in pathogenic versus non-pathogenic species. Overall, these data provide useful insights to the elucidation of differences in clinical relevance among *Acinetobacter* species.

Acknowledgements

References

1. Dijkshoorn L, Nemec A, Seifert H (2007) An increasing threat in hospitals: multidrug resistant *Acinetobacter baumannii*. Nat Rev Microbiol 5: 939-951.

2. Peleg AY, Seifert H, Paterson DL (2008) *Acinetobacter baumannii*: emergence of a successful pathogen. Clin Microbiol Rev 21: 538-582.

3. Nemec A, Krizova L, Maixnerova M, van der Reijden TJ, Deschaght P, et al. Genotypic and phenotypic characterization of the *Acinetobacter calcoaceticus-Acinetobacter baumannii* complex with the proposal of *Acinetobacter pittii* sp. nov. (formerly *Acinetobacter* genomic species 3) and *Acinetobacter nosocomialis* sp. nov. (formerly *Acinetobacter* genomic species 13TU). Res Microbiol 162: 393-404.

4. Chiang MC, Kuo SC, Chen SJ, Yang SP, Lee YT, et al. Clinical characteristics and outcomes of bacteremia due to different genomic species of *Acinetobacter baumannii* complex in patients with solid tumors. Infection.

5. Chuang YC, Sheng WH, Li SY, Lin YC, Wang JT, et al. Influence of genospecies of *Acinetobacter baumannii* complex on clinical outcomes of patients with acinetobacter bacteremia. Clin Infect Dis 52: 352-360.

6. Koh TH, Tan TT, Khoo CT, Ng SY, Tan TY, et al. *Acinetobacter calcoaceticus- Acinetobacter baumannii* complex species in clinical specimens in Singapore. Epidemiol Infect: 1-4.

7. Turton JF, Shah J, Ozongwu C, Pike R Incidence of *Acinetobacter* species other than *A. baumannii* among clinical isolates of *Acinetobacter*: evidence for emerging species. J Clin Microbiol 48: 1445-1449.

8. Van den Broek PJ, van der Reijden TJ, van Strijen E, Helmig-Schurter AV, Bernards AT, et al. (2009) Endemic and epidemic *Acinetobacter* species in a university hospital: an 8-year survey. J Clin Microbiol 47: 3593-3599.

9. Yum JH, Yi K, Lee H, Yong D, Lee K, et al. (2002) Molecular characterization of metallo-beta-lactamase-producing *Acinetobacter baumannii* and *Acinetobacter* genomospecies 3 from Korea: identification of two new integrons carrying the bla(VIM-2) gene cassettes. J Antimicrob Chemother 49: 837-840.

10. Villegas MV, Hartstein AI (2003) *Acinetobacter* outbreaks, 1977-2000. Infect Control Hosp Epidemiol 24: 284-295.

11. Wendt C, Dietze B, Dietz E, Ruden H (1997) Survival of *Acinetobacter baumannii* on dry surfaces. J Clin Microbiol 35: 1394-1397.

12. Jawad A, Seifert H, Snelling AM, Heritage J, Hawkey PM (1998) Survival of *Acinetobacter baumannii* on dry surfaces: comparison of outbreak and sporadic isolates. J Clin Microbiol 36: 1938-1941.

13. Cerqueira GM, Peleg AY Insights into *Acinetobacter baumannii* pathogenicity. IUBMB Life.

14. Eijkelkamp BA, Hassan KA, Paulsen IT, Brown MH Investigation of the human pathogen *Acinetobacter baumannii* under iron limiting conditions. BMC Genomics 12: 126.

15. Mussi MA, Gaddy JA, Cabruja M, Arivett BA, Viale AM, et al. The opportunistic human pathogen *Acinetobacter baumannii* senses and responds to light. J Bacteriol 192: 6336-6345.

16. O'Toole GA, Kolter R (1998) Flagellar and twitching motility are necessary for *Pseudomonas aeruginosa* biofilm development. Mol Microbiol 30: 295-304.

17. Kapoor S, Panda D (2009) Targeting FtsZ for antibacterial therapy: a promising avenue. Expert Opin Ther Targets 13: 1037-1051.

18. Tomaras AP, Dorsey CW, Edelmann RE, Actis LA (2003) Attachment to and biofilm formation on abiotic surfaces by *Acinetobacter baumannii*: involvement of a novel chaperone-usher pili assembly system. Microbiology 149: 3473-3484.

19. Dorsey CW, Tomaras AP, Connerly PL, Tolmasky ME, Crosa JH, et al. (2004) The siderophore-mediated iron acquisition systems of *Acinetobacter baumannii* ATCC 19606 and *Vibrio anguillarum* 775 are structurally and functionally related. Microbiology 150: 3657-3667.

20. Yamamoto S, Okujo N, Sakakibara Y (1994) Isolation and structure elucidation of acinetobactin, a novel siderophore from *Acinetobacter baumannii*. Arch Microbiol 162: 249-254.

21. Horvath P, Barrangou R CRISPR/Cas, the immune system of bacteria and archaea. Science 327: 167-170.

22. Makarova KS, Haft DH, Barrangou R, Brouns SJ, Charpentier E, et al. Evolution and classification of the CRISPR-Cas systems. Nat Rev Microbiol 9: 467-477.

23. Hubbard BK, Koch M, Palmer DR, Babbitt PC, Gerlt JA (1998) Evolution of enzymatic activities in the enolase superfamily: characterization of the (D)-glucarate/galactarate catabolic pathway in *Escherichia coli*. Biochemistry 37: 14369-14375.

24. Lamichhane-Khadka R, Frye JG, Porwollik S, McClelland M, Maier RJ Hydrogen-stimulated carbon acquisition and conservation in *Salmonella enterica serovar Typhimurium*. J Bacteriol 193: 5824-5832.

25. Camarena L, Bruno V, Euskirchen G, Poggio S, Snyder M Molecular mechanisms of ethanol-induced pathogenesis revealed by RNA-sequencing. PLoS Pathog 6: e1000834.

26. De Breij A, Dijkshoorn L, Lagendijk E, van der Meer J, Koster A, et al. Do biofilm formation and interactions with human cells explain the clinical success of *Acinetobacter baumannii*? PLoS One 5: e10732.

27. Karah N, Haldorsen B, Hegstad K, Simonsen GS, Sundsfjord A, et al. Species identification and molecular characterization of *Acinetobacter* spp. blood culture isolates from Norway. J Antimicrob Chemother 66: 738-744.

28. Choi SH, Choo EJ, Kwak YG, Kim MY, Jun JB, et al. (2006) Clinical characteristics and outcomes of bacteremia caused by *Acinetobacter* species other than *A. baumannii*: comparison with *A. baumannii* bacteremia. J Infect Chemother 12: 380-386.

29. Dorsey CW, Beglin MS, Actis LA (2003) Detection and analysis of iron uptake components expressed by *Acinetobacter baumannii* clinical isolates. J Clin Microbiol 41: 4188-4193.

30. De Breij A, Gaddy J, van der Meer J, Koning R, Koster A, et al. (2009) CsuA/BABCDE-dependent pili are not involved in the adherence of *Acinetobacter baumannii* ATCC19606(T) to human airway epithelial cells and their inflammatory response. Res Microbiol 160: 213-218.

31. Lamarche MG, Wanner BL, Crepin S, Harel J (2008) The phosphate regulon and bacterial virulence: a regulatory network connecting phosphate homeostasis and pathogenesis. FEMS Microbiol Rev 32: 461-473.

32. Boom R, Sol CJ, Salimans MM, Jansen CL, Wertheim-van Dillen PM, et al. (1990) Rapid and simple method for purification of nucleic acids. J Clin Microbiol 28: 495-503.

33. Lennon NJ, Lintner RE, Anderson S, Alvarez P, Barry A, et al. A scalable, fully automated process for construction of sequence-ready barcoded libraries for 454. Genome Biol 11: R15.

34. Enright AJ, Van Dongen S, Ouzounis CA (2002) An efficient algorithm for large-scale detection of protein families. Nucleic Acids Res 30: 1575-1584.

35. Chenna R, Sugawara H, Koike T, Lopez R, Gibson TJ, et al. (2003) Multiple sequence alignment with the Clustal series of programs. Nucleic Acids Res 31: 3497-3500.

36. Kumar S, Nei M, Dudley J, Tamura K (2008) MEGA: a biologist-centric software for evolutionary analysis of DNA and protein sequences. Brief Bioinform 9: 299-306.

37. Salgado H, Moreno-Hagelsieb G, Smith TF, Collado-Vides J (2000) Operons in *Escherichia coli*: genomic analyses and predictions. Proc Natl Acad Sci U S A 97: 6652-6657.

38. Wang L, Trawick JD, Yamamoto R, Zamudio C (2004) Genome-wide operon prediction in *Staphylococcus aureus*. Nucleic Acids Res 32: 3689-3702.

39. Bochner BR (2009) Global phenotypic characterization of bacteria. FEMS Microbiol Rev 33: 191-205.

40. Biondi EG, Tatti E, Comparini D, Giuntini E, Mocali S, et al. (2009) Metabolic capacity of *Sinorhizobium (Ensifer) meliloti* strains as determined by phenotype MicroArray analysis. Appl Environ Microbiol 75: 5396-5404.

41. Hammer OH, David A.T., Ryan, PD. (2001) PAST: Paleontological Statistics Software Package for Education and Data Analysis. Palaeontologia Electronica 4: 9.

42. El Ghalbzouri A, Commandeur S, Rietveld MH, Mulder AA, Willemze R (2009) Replacement of animal-derived collagen matrix by human fibroblast-derived dermal matrix for human skin equivalent products. Biomaterials 30: 71-78.

43. Lee JC, Koerten H, van den Broek P, Beekhuizen H, Wolterbeek R, et al. (2006) Adherence of *Acinetobacter baumannii* strains to human bronchial epithelial cells. Res Microbiol 157: 360-366.

44. Dijkshoorn L, Brouwer CP, Bogaards SJ, Nemec A, van den Broek PJ, et al. (2004) The synthetic N-terminal peptide of human lactoferrin, hLF(1-11), is highly effective against experimental infection caused by multidrug-resistant *Acinetobacter baumannii*. Antimicrob Agents Chemother 48: 4919-4921.

45. Piechaud D, Piechaud, M., Second, L. (1951) Etude de 26 souches de *Moraxella Iwoffi*. Ann Inst Pasteur 80: 97-99.

46. Adams MD, Goglin K, Molyneaux N, Hujer KM, Lavender H, et al. (2008) Comparative genome sequence analysis of multidrug-resistant *Acinetobacter baumannii*. J Bacteriol 190: 8053-8064.

47. Fournier PE, Vallenet D, Barbe V, Audic S, Ogata H, et al. (2006) Comparative genomics of multidrug resistance in *Acinetobacter baumannii*. PLoS Genet 2: e7.

48. Iacono M, Villa L, Fortini D, Bordoni R, Imperi F, et al. (2008) Whole-genome pyrosequencing of an epidemic multidrug-resistant *Acinetobacter baumannii* strain belonging to the European clone II group. Antimicrob Agents Chemother 52: 2616-2625.

49. Barbe V, Vallenet D, Fonknechten N, Kreimeyer A, Oztas S, et al. (2004) Unique features revealed by the genome sequence of *Acinetobacter* sp. ADP1, a versatile and naturally transformation competent bacterium. Nucleic Acids Res 32: 5766-5779.

50. Vallenet D, Engelen S, Mornico D, Cruveiller S, Fleury L, et al. (2009) MicroScope: a platform for microbial genome annotation and comparative genomics. Database (Oxford) 2009: bap021.

51. De Breij A, Haisma EM, Rietveld M, El Ghalbzouri A, van den Broek PJ, et al. (2012) Three-dimensional human skin equivalent as a tool to study *Acinetobacter baumannii* colonization. Antimicrob Agent Chemother 56: 2459-2464.

chapter 5